Evaluation of the Bayesian Downscaling Algorithm for Achieving Higher Resolution Soil Moisture Data

Xiaoling Wu, Jeffrey P. Walker, Nan Ye

***Abstract*—The NASA-launched Soil Moisture Active Passive satellite mission (SMAP) had the objective to globally characterize soil moisture with an intermediate resolution (9 km), through the integration of radar (3 km) and radiometer (36 km) observations. The SMAP team has evaluated various downscaling techniques to achieve this goal. This study examined the performance of an additional downscaling technique, the Bayesian merging method, as an alternative candidate approach. This method breaks from the standard linear downscaling techniques of SMAP, opting instead for a more innovative approach based on Bayes' Theorem. Here the intermediate resolution soil moisture is achieved via the incorporation of a background estimate, which is refined through comparison between observed and predicted brightness temperatures and backscatter coefficients that link the high and low-resolution data. However, it is crucial to assess the robustness of the Bayesian method using actual satellite observations, in addition to its prior evaluation using synthetic datasets. The fourth Soil Moisture Active Passive Experiment (SMAPEx-4), conducted in Australia, represented the sole occasion for concurrent high-resolution airborne observations during operation of the SMAP radar. As such, this study employed the Bayesian algorithm using the SMAP datasets throughout the SMAPEx-4 period. Downscaled soil moisture products from this method, as well as from the official baseline and enhancement techniques, were compared. The average RMSE and R^2 of the 9 km downscaled soil moisture were found to be 0.035 cm^3/cm^3 and 0.55 for the Bayesian method, 0.093 cm^3/cm^3 and 0.35 for the baseline, and 0.069 cm^3/cm^3 and 0.41 for the enhancement method.**

***Index Terms*—SMAPEx, soil moisture retrieval, resolution improvement, active and passive.**

I. INTRODUCTION

SOIL moisture data at a medium resolution of approximately 9 km on a global scale can greatly contribute to various hydrological and meteorological applications, such as flood forecasting, drought assessment, weather forecasting, and agriculture administration [1]. The primary challenge in utilizing remote sensing technologies for soil moisture measurement lies in balancing the trade-off between resolution and radiometric precision. While microwave radiometry is widely recognized as the most effective technique for accurately retrieving surface soil moisture, its low resolution of approximately 40 km restricts its usage for regional-scale applications [2, 3]. Conversely, the radar microwave sensing technique, which boasts a higher resolution being better than 3 km, often struggles to accurately retrieve global soil moisture because of the high level of noise. Consequently, the Soil Moisture Active Passive (SMAP) mission of NASA aimed to address the limitations of both the radar and radiometer technologies by incorporating both into its design. This combination was intended to result in soil moisture products of intermediate resolution, being approximately 9 km [4, 5].

Apart from radar, high resolution data from other sensors including optical and thermal also offers a potential solution to disaggregating large pixels into smaller ones [6-8]. Moreover, additional information on factors controlling soil moisture variability, such as soil properties, vegetation characteristics, or meteorological observations could be used to disaggregate the low resolution passive microwave observations, using either physical models or empirical relationships [9]. However, intermediate resolution soil moisture retrievals from the above mentioned downscaling algorithms are limited by the availability of the soil and vegetation properties required as inputs by the methods at global scale and high resolution. It should also be noted that the use of optical data is limited to clear sky conditions, while the active-passive microwave approach has the advantage of being applicable under all weather conditions.

The active-passive method is commonly implemented through the integration of both radiometer and radar data utilizing a linear downscaling technique. Two methodologies, namely the SMAP official baseline algorithm and the optional downscaling algorithm, have been put forward as potential solutions [10, 11]. These methods, in conjunction with an additional linear downscaling method referred to as the change detection method [12], were assessed using pre-launch data [13]. Comparison of those methods indicated that the optional downscaling method produced the most favourable outcome in terms of retrieving soil moisture at an intermediate resolution. Given that all three active-passive downscaling algorithms are linear in nature, relying on the premise of linear correlation between passive and active data, it is advisable to evaluate other possible active-passive combination approaches for the SMAP mission.

One such alternative is the Bayesian merging method, which uses a nonlinear approach to retrieve soil moisture at medium resolution [14]. Such evaluations should be conducted within a comparable experimental framework to

xxxxxxxxx

Xiaoling Wu is with Department of Civil Engineering, Monash University, Australia (e-mail: xiaoling.wu@monash.edu).

Jeffrey P. Walker is with Department of Civil Engineering, Monash University, Australia (e-mail: jeff.walker@monash.edu).

Nan Ye is with Department of Civil Engineering, Monash University, Australia (e-mail: nan.ye@monash.edu).

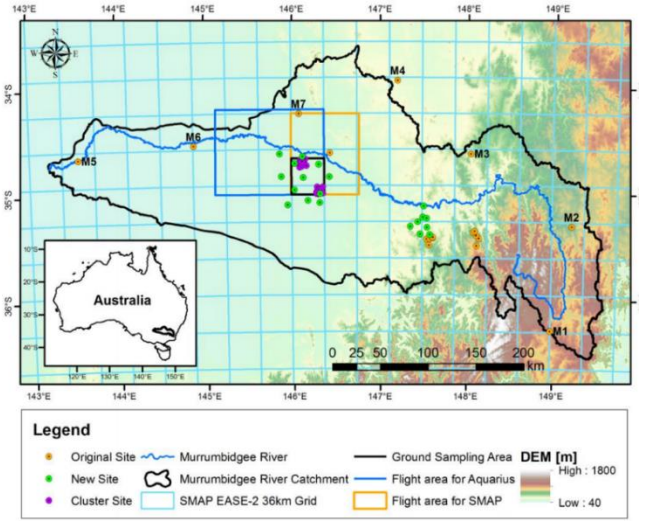

Figure 1: Location and coverage of the SMAPEx-4 field campaign. The campaign was conducted in Yanco, NSW Australia from 1-22 May 2015. The flight area (in orange) for SMAP is ~72 km x 85 km. Rectangle in black with the size of ~36 km x 36 km is the main study area where the ground sampling activities were conducted.

ensure a fair comparison of results. According to [14] the Bayesian method demonstrated encouraging outcomes in the retrieval of soil moisture at the resolution of 9 km, with a Root-Mean-Square-Error (RMSE) of 0.027 cm^3/cm^3 when utilizing synthetic data with low-level noise, and 0.044 cm^3/cm^3 when utilizing synthetic data with high-level noise. The low- (0.1 – 1.0 dB) and high-level (1.0 – 2.0 dB) scenarios were simulated due to limited knowledge about actual radar noise levels. However, the development and implementation of the synthetic data used in [14] were based on numerous assumptions that may not be thoroughly justified. Hence, the aim of the current study was to assess the validity of the Bayesian method using actual observations from the SMAP satellite's radar and radiometer data. This was achieved through comparison with the officially released SMAP downscaled products, including those obtained through the baseline algorithm and the resolution enhancement method.

II. Data Set and Study Area

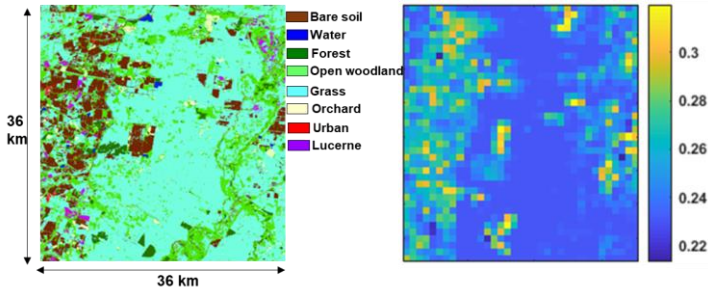

Figure 2: Map of land use (left) and map of surface roughness *h* (right) for the SMAPEx-4 study area.

As listed in Table 1, two main data sets were used in this study: the actual SMAP radar and radiometer data, and the field data obtained from the extensive field campaign in NSW Australia, namely the 4th Soil Moisture Active Passive Experiment (SMAPEx-4). Accordingly, the satellite data analyzed in this study were acquired in May 2015, during the period when the SMAP radar sensor was still operational, allowing the Bayesian downscaling technique to be assessed using seven days of airborne observations: 2nd, 5th, 10th, 11th, 18th, 19th, and 21st of May 2015.

The SMAP data used includes the 36 km resolution brightness temperature *(Tb)* from the radiometer at *h*-pol and *v*-pol and its retrieved soil moisture at the same resolution, the 3 km resolution backscatter (σ) from the radar at *hh*-pol, *vv*-pol and *hv*-pol, the retrieved soil moisture at the same resolutions, the ancillary data used for both the radar and radiometer retrieval models, the active-passive downscaled 9 km soil moisture product, and the Backus-Gilbert enhanced soil moisture product posted onto the 9 km grid. The ancillary data utilized in this study encompass the vegetation parameters such as vegetation water content (*VWC*) and the parameter *b* that is dependent on the type of vegetation, surface roughness parameter *h*, and surface temperature T_{surf}, all of which are incorporated in the forward modelling of brightness temperature and backscatter within the context of the Bayesian downscaling framework. It is noteworthy to mention that the accuracy of these parameters has the potential to impact the accuracy of the downscaled soil moisture produced.

The field data, used here as the reference data only, was collected from the SMAPEx-4 field campaign conducted in the township of Yanco in New South Wales in Australia from 1 May to 22 May 2015 (Figure 1). The SMAPEx field campaign was crafted with the objective of acquiring airborne microwave data including active and passive observations, along with ground collected soil moisture data and any relevant ancillary parameters, during SMAP overpasses. This was done to provide reference observations of both microwave and soil moisture data for the SMAP mission.

The study site was chosen for SMAPEx due to its favourable conditions, including a flat topography, widespread availability of in-situ stations for soil moisture monitoring, and its representation of typical surface conditions such as soil type, vegetation, and land use found in semi-arid environments. Maps of land use and surface roughness are shown in Figure 2. The site is situated within the grazing and semi-arid agricultural region of the Murrumbidgee River catchment of south-eastern Australia and is part of the broader Murray-Darling basin. Descriptions of the SMAPEx site and its monitoring schedules can be found from [15], with complete details of the experimental workplan available on the experiment website (www.smapex.monash.edu.au). Airborne observations collected during SMAPEx-4 covered an area equivalent to four SMAP-sized radiometer footprints, which measured approximately 71 km × 85 km at that latitude. Please note that only results on the black rectangle in Figure 1 (with a size of ~36 km × 36 km) are shown and discussed in the following sections, as this is the area where the ground sampling activities had taken place.

The main sources of field data utilized in this study include the airborne observations obtained from the Polarimetric L-band Multibeam Radiometer (PLMR). These data included brightness temperature at both *h*- and *v*-polarization, with a resolution of 1 km, as well as the derived soil moisture. Both the observed brightness temperature and the inversed soil moisture data were further aggregated to 3 km resolution and 9 km resolution in order to evaluate the performance of the downscaling algorithm at these resolutions. This retrieved soil moisture from PLMR has been validated against the ground soil moisture which was collected using a handheld instrument (Hydraprobe Data Acquisition System) at 250 m resolution. The airborne data underwent a series of processing steps, including calibration, temperature correction, and angle normalization, to serve as a reference dataset prototype for the SMAP mission [16]. Ancillary parameters regarding the vegetation, surface roughness, surface temperature and etc were also used here for soil moisture retrieval from the PLMR observations.

III. Methodology

The total area consists of approximately four SMAP radiometer footprints. The Bayesian downscaling procedure was implemented for each footprint and a brief overview is provided here, with comprehensive information provided in [14]. Within each 36 km × 36 km area the optimal soil moisture estimates, $\theta(F)$, at a given resolution "F" (in this study, either 3 km or 9 km) can be calculated from an initial background soil moisture estimate, θ_b, using the Kalman filter update equation [17]. Accordingly, this background estimate is updated based on the discrepancy between the observation Z and the estimated observation (brightness temperature and backscatter) given by $h([\theta_b])$, as seen in the following practical application of Bayes' Theorem:

$$[\theta(F)] = [\theta_b] + [K] \times \{[Z] - h([\theta_b])\}. \quad (1)$$

Figure 3 shows a flowchart of this downscaling method. The final retrieved soil moisture $[\theta(F)]$ is a vector of values for each 3 km pixel within a SMAP radiometer footprint in the study area. Meanwhile, $[\theta_b]$, denoting the vector of background soil moisture, is also represented in the same manner, at each 3 km pixel within the same footprint.

The $[\theta_b]$ can be obtained through two alternative approaches, which have been evaluated in this implementation. The first is obtained from the 36 km resolution SMAP Tb_h, via a single-channel passive microwave retrieval method [18-19]. The second source is acquired from the 3 km resolution SMAP backscatter that utilizes a fusion of three active microwave retrieval models [20-22].

The observation function, $h([\theta_b])$, considers the soil covered

Table 1

Summary of datasets used in this study, including data from the SMAP satellite and from the SMAPEx-4 field campaign in Australia during May 2015.

Name	Resolution	Description	Source of data
SMAP Tb_h, Tb_v	36 km	Brightness temperature at *h*- and *v*-pol	SMAP L1B_TB
SMAP σ_{hh}, σ_{vv}, σ_{hv}	3 km	Radar sigma0 at *hh*-, *vv*- and *hv*-pol	SMAP L1A_Radar
SMAP_SM_A	3 km	Radar soil moisture	SMAP L2_SM_A
SMAP_SM_P	36 km	Radiometer soil moisture	SMAP L2_SM_P
SMAP_SM_AP	9 km	SMAP active-passive soil moisture	SMAP L2_SM_AP
SMAP_SM_P_E	9 km	SMAP radiometer enhancement soil moisture	SMAP L2_SM_P_E
SMAP ancillary data	3 km	SMAP *VWC, b, h,* T_{surf}	SMAP L2_SM_A
PLMR Tb_h, Tb_v	1, 3, 9 km	SMAPEx-4 PLMR brightness temperature at *h*- and *v*-pol	SMAPEx-4
PLMR SM	1, 3, 9 km	SMAPEx-4 PLMR soil moisture	SMAPEx-4
SMAPEx-4 SM	250 m	SMAPX-4 ground sampled soil moisture	SMAPEx-4
SMAPEx-4 ancillary data	1 km	SMAPEx-4 *VWC, b, h,* T_{surf}	SMAPEx-4

by vegetation, and so predicts the brightness temperature and backscatter using the forward models with the background soil moisture on a 3 km resolution grid. In terms of [*Z*], it contains SMAP observations including 36 km resolution brightness temperature at *h*- and *v*-pol, as well as 3 km resolution backscatter σ at *hh*, *vv*, and *hv*-pol. The Kalman gain, [*K*], is derived from uncertainties in the observations and the background states through

$$[K] = [P][H^T] / ([H][P][H^T] + [R]), \quad (2)$$

where the matrix [*P*] symbolizes the error covariance of the background soil moisture, the matrix [*R*] symbolizes the error covariance of the observations, and the matrix [*H*] is the linear form of the function *h*([ ]) that relates the observations vector to the background state vector. Here [*P*] was estimated through two methods: i) by comparing the background soil moisture vector [θ_b] to the reference soil moisture from the airborne PLMR sensor, or ii) as the difference between SMAP radar-based background and SMAP radiometer-based background soil moisture. The comparison of results from both methods aimed to determine assess the practical approach for estimating [*P*] in an operational context from the second approach, with those of the best available estimate from the first approach. As [*R*] is founded on the instrument parameters and the precision of the data processing, particularly the accuracy of calibration as outlined in the SMAP Algorithm Theoretical Basis Documents. Moreover, [*H*] was represented by the first derivative (Jacobian) of the observation function *h*([θ_b])

$$[H] = \delta h([\theta_b]) / \delta[\theta]. \quad (3)$$

For a single pixel-wise implementation, the vector [*Z*] encompasses 434 observations in this study, including two SMAP brightness temperatures at 36 km being *h*- and *v*-pol, and backscatter at three polarisations including *hh*-, *vv*- and *hv*-pol taken at each of the 144 3 km × 3 km pixels. The elements of the observation vector [*Z*], the predicted observation vector *h*([θ_b]), and the matrix [*H*] are represented as follows:

$$[Z] = [Tb_h\ Tb_v\ \sigma_{hh,1}\ \sigma_{vv,1}\ \sigma_{hv,1} \dots \sigma_{hh,144}\ \sigma_{vv,144}\ \sigma_{hv,144}]^T_{434\times1} \quad (4)$$

$$h([\theta]) = [Tb_h(\theta_b)\ Tb_v(\theta_b)\ \sigma_{hh,1}(\theta_b)\ \sigma_{vv,1}(\theta_b)\ \sigma_{hv,1}(\theta_b)^T \dots \sigma_{hh,144}(\theta_b)\ \sigma_{vv,144}(\theta_b)\ \sigma_{hv,144}(\theta_b)]_{434\times1} \quad (5)$$

$$[H] = \begin{bmatrix} \delta Tb_h/\delta\theta_{f,1} & \cdots & \delta Tb_h/\delta\theta_{f,144} \\ \vdots & \ddots & \vdots \\ \delta\sigma_{hv,144}/\delta\theta_{f,1} & \cdots & \delta\sigma_{hv,144}/\delta\theta_{f,144} \end{bmatrix}^T_{434\times144.} \quad (6)$$

$$[P] = \begin{bmatrix} \theta_{b\_P-}\theta_{b\_A,1} & \cdots & 0 \\ \vdots & \ddots & \vdots \\ 0 & \cdots & \theta_{b\_P-}\theta_{b\_A,144} \end{bmatrix}^T_{144\times144.} \quad (7)$$

In Eq. (4)-(6), Each SMAP radiometer footprint consists of 144 3 km × 3 km pixels, with a total of 434 observations made for each footprint. These observations include one brightness temperature measurement for both *h*- and *v*- polarizations, as well as 144 backscatter measurements for each of the three polariszations *hh*-, *vv*-, and *hv*. The error covariance of the background soil moisture field constituted the 144 diagonal values of [P], while zeros were assigned to all off diagonal elements as shown in Eq. (7), with the assumption of uncorrelated soil moisture error among the 3 km pixels. In terms of the matrix [R], the 434 diagonal elements were set as the observation accuracy of SMAP for the passive (1.3 K for both *h*- and *v*-pol) and active data (1 dB for *hh*-, and *vv*-pol, 1.5 dB for *hv-pol*) while the off diagonal elements were also assigned zeros, with the assumption that observation errors were independent of each other in both spatial and polarisation domains.

The resulting soil moisture values obtained through the downscaling process [$\theta(F)$] were compared to the soil moisture reference map with a resolution of 3 km, derived from high-resolution PLMR observations with a resolution of 1 km [23]. The Bayesian algorithm's performance was then assessed by comparing its results to the SMAP baseline algorithm in [13], and the SMAP resolution enhancement method. The SMAP resolution enhancement method is based on the Backus-Gilbert optimal interpolation technique which utilises the information contained in the oversampling to produce a slightly enhanced spatial resolution (27 km rather than 36 km), and posted onto a 9 km grid. Accordingly, the accuracy of this product at an assumed 9 km spatial resolution was assessed, along with the downscaled results at a 9 km. Two distinct approaches can be used to obtain the downscaled results at 9 km resolution: (i) by linearly upscaling the downscaled data from 3 km to 9 km resolution, and (ii) by utilizing the SMAP radar backscatter aggregated to 9 km resolution directly as the input of [*Z*]. The performance of both approaches was evaluated.

The Bayesian algorithm present here have been previously studied by [14] and [24]. [14] has shown the feasibility of this algorithm for acquiring medium-resolution soil moisture product by using synthetic radar and radiometer data; while [24] evaluated the same approach but using data from SMAPEx-3 field campaign. Data from SMAPEx-3 2011 were firstly processed to mimic SMAP data (which were not launched by then) and then analysis was performed on different soil moisture retrieval methods. But in this paper, the novelty is that it is the first ever evaluation of Bayesian downscaling algorithm using real SMAP radiometer and radar data. Reference data from SMAPEx-4 2015 provided the only opportunity while SMAP radar was still functioning and therefore worth investigating of the Bayesian algorithm with such realistic satellite data.

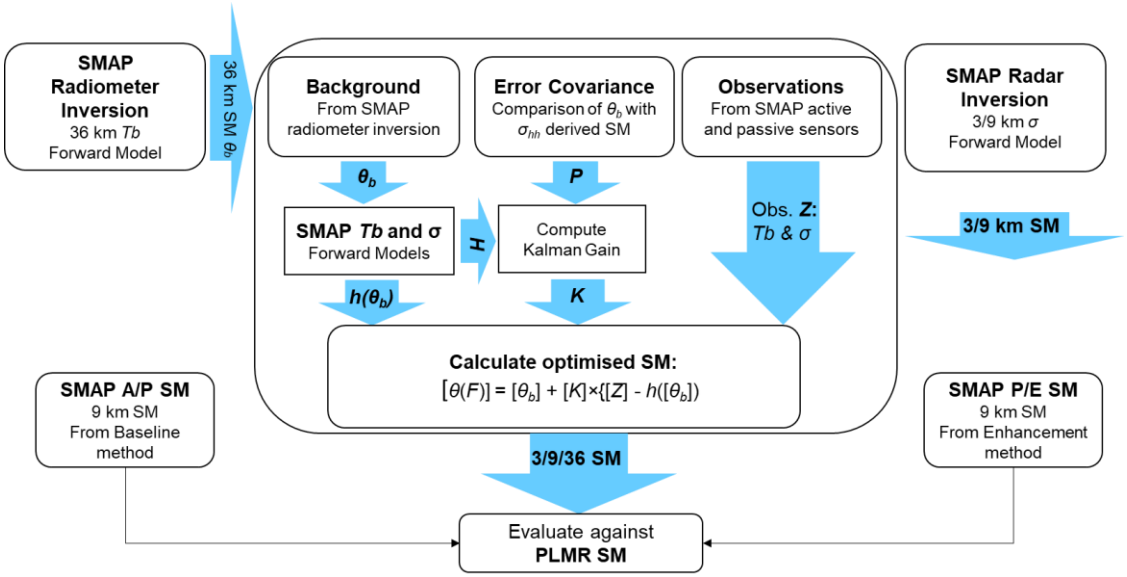

Figure 3: Flowchart of the Bayesian downscaling method.

IV. Results and Discussion

A. Estimation of the background soil moisture field

Estimating the background soil moisture was achieved by directly inverting either i) the 36 km resolution SMAP brightness temperature or ii) the 3 km resolution SMAP backscatter. Thus, there are four different sources for estimating the background field: from the 36 km SMAP brightness temperature and SMAP ancillary data (Type 1); from 3 km SMAP radar and SMAP ancillary data (Type 2); from 36 km SMAP radiometer and actual ground ancillary data (SMAPEx field data; Type 3); or from 3 km SMAP radar and actual ground ancillary data (Type 4). The soil moisture values for Type 1 and Type 2 were obtained directly from SMAP published products, while the background soil moisture value for Type 3 was calculated in this study from *h*-pol *Tb* utilizing the single channel τ-ω model [19], and the soil moisture value for Type 4 was computed using the active retrieval model, as described in [14], based on *hh*-pol backscatter. Comparison between Type 1 and Type 3 background fields across the seven days is displayed in Table 1. An example of the SMAP radar observation and the retrieved soil moisture on D1, D4, and D7 (D refers to day) is illustrated in Figure 4. The spatial variation in surface roughness (as shown in Figure 2) and vegetation structural characteristics have been shown to have a notable impact on the accuracy of soil moisture retrievals using the active remote sensing. Therefore, it is crucial to consider these factors when estimating soil moisture at a fine spatial resolution through downscaling, as their effects can propagate through the retrieval process and potentially result in substantial errors in the derived soil moisture values.

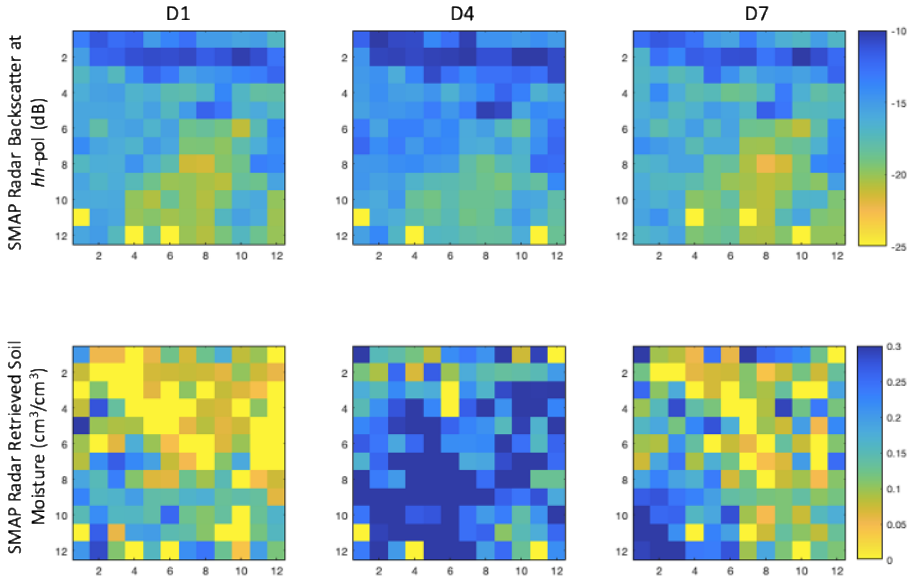

Figure 4: The 3 km resolution SMAP radar backscatter at *hh*-pol on D1, D4 and D7 together with the soil moisture (cm^3/cm^3) maps derived from those backscatter data.

Table 2

Time series of observed brightness temperature (*Tb*, in K) and estimated brightness temperature (from radiometer inversed background soil moisture) at *h*-pol and *v*-pol at 36 km resolution, and their first derivatives (Jacobian) across the 7 days of the airborne campaign. Also shown are the background soil moisture values (cm^3/cm^3) retrieved via the single channel passive microwave retrieval method, including Background soil moisture #1: from 36 km SMAP radiometer and SMAP ancillary data (Type 1); and Background soil moisture #3: from 36 km SMAP radiometer and actual ground ancillary data (SMAPEx field data; Type 3).

	D1	**D2**	**D3**	**D4**	**D5**	**D6**	**D7**
Observed Tb_h (K)	251	244	230	205	217	240	250
Observed Tb_v (K)	274	263	252	241	248	265	273
Estimated Tb_h (K)	262	255	243	233	234	248	263
Estimated Tb_v (K)	282	270	269	264	267	269	282
Jacobian of Tb_h ($K/(cm^3/cm^3)$)	-271	-251	-220	-192	-222	-265	-280
Jacobian of Tb_v ($K/(cm^3/cm^3)$)	-131	-145	-128	-141	-149	-151	-122
Background soil moisture #1 (cm^3/cm^3)	0.100	0.123	0.203	0.261	0.23	0.166	0.09
Background soil moisture #3 (cm^3/cm^3)	0.089	0.097	0.175	0.196	0.195	0.136	0.077

Table 3

Time series of observed brightness temperature (*Tb*, in K) and estimated brightness temperature (from forward model using 3 km radar inversed background soil moisture) at *h*-pol and *v*-pol at 36 km resolution, and their first derivatives (Jacobian) across 7 days. Also shown are average soil moisture values (cm^3/cm^3) estimated from radar backscatter (σ_{hh}).

	D1	D2	D3	D4	D5	D6	D7
Observed Tb_h (K)	251	244	230	205	217	240	250
Observed Tb_v (K)	274	263	252	241	248	265	273
Estimated Tb_h (K)	243	237	225	216	220	231	234
Estimated Tb_v (K)	272	265	260	250	257	272	264
Jacobian of Tb_h ($K/(cm^3/cm^3)$)	-217	-202	-170	-147	-144	-189	-197
Jacobian of Tb_v ($K/(cm^3/cm^3)$)	-145	-142	-132	-128	-135	-148	-143
Background soil moisture (cm^3/cm^3)	0.127	0.149	0.222	0.268	0.241	0.187	0.159

Type 1 and Type 2 background soil moisture data are discussed in the following context. First the most appropriate background soil moisture value was selected between the active and passive soil moisture retrieval models. Next [*P*] was calculated as the error covariance by comparing the background soil moisture against the reference soil moisture obtained from PLMR.

Utilizing the background soil moisture obtained from the SMAP radiometer or SMAP radar, the *Tb* and σ were then calculated through the forward models. Their first derivatives (Jacobian) were also calculated accordingly. Table 2 shows the time series of the estimated T_b and associated Jacobians across the 7 days of the field campaign, with the estimated σ and Jacobian on D1 illustrated as an example in Figure 5, when the SMAP radiometer inversed soil moisture at 36 km was used as the background field. Consequently, by comparing to the observed brightness temperature the RMSE of the estimated brightness temperature was around 14 K at *h*-pol and 13 K at *v*-pol across the 7 days; and the RMSE of the estimated backscatter was approximately 2.9 dB at *hh*-pol, 2.1 dB at *vv*-pol and 12.6 dB at *hv*-pol. In contrast, Table 3 displays the changes of estimated *Tb* and their Jacobians across the 7 days; the estimated σ and Jacobian on D4 are presented in Figure 6 as an example, when the SMAP radar-derived soil moisture at 3 km was taken as the background. The RMSE of the estimated brightness temperature in this circumstance was found to be higher, at approximately 10 K at *h*-pol and 8 K at *v*-pol, and the RMSE of the estimated backscatter was approximately 3.6 dB at *hh*-pol, 3.0 dB at *vv*-pol and 14.1 dB at *hv*-pol, than when adopting the radiometer inversed soil moisture as the background.

Evaluation on all seven days was conducted, with consistent results obtained for each day. Figures 5-7 presents the results obtained for day D1 as an example. When the background soil moisture inversed from the SMAP radiometer, the 9 km resolution RMSE against the reference soil moisture on D1 was 0.021 cm^3/cm^3. The correlation coefficient between the downscaled and reference soil moisture was approximately 0.38. Conversely, when using the background soil moisture retrieved from the SMAP radar, the resulting RMSE was 0.165 cm^3/cm^3, which is higher than when using the soil moisture inversed from the radiometer. The correlation coefficient (R^2) in this case was approximately 0.11. Similar to the findings on D1, the results on other days also demonstrated that background soil moisture from the SMAP radiometer yielded much higher accuracy in downscaled soil moisture compared to that from the SMAP radar. The inadequate performance from the radar-based estimation of soil moisture may be due to the use of SMAP's default ancillary parameters for retrieval and forward estimation, resulting in an inaccurate background soil moisture. Consequently, based on the comparison of these two methods, the SMAP radiometer for background soil moisture retrieval was selected for further assessment of the Bayesian downscaling approach.

B. Downscaling performance and discussion

The analysis conducted above indicated that the SMAP radiometer retrieval of soil moisture provided the most suitable soil moisture background for the subsequent predictions of brightness temperature and backscatter values. Therefore, this method was chosen for further modelling and analysis. The error covariance [*P*] was calculated by comparing the soil moisture estimates retrieved from both the radiometer and radar methods, since the actual soil moisture measurements were not available for the SMAP application. A comparison was conducted between the estimated [*P*] and the "true" [*P*] obtained from the difference between the background and reference maps. This comparison allowed for a more rigorous evaluation of the accuracy of the background soil moisture used in the SMAP analysis. The average difference between the RMSE of the estimated and "true"

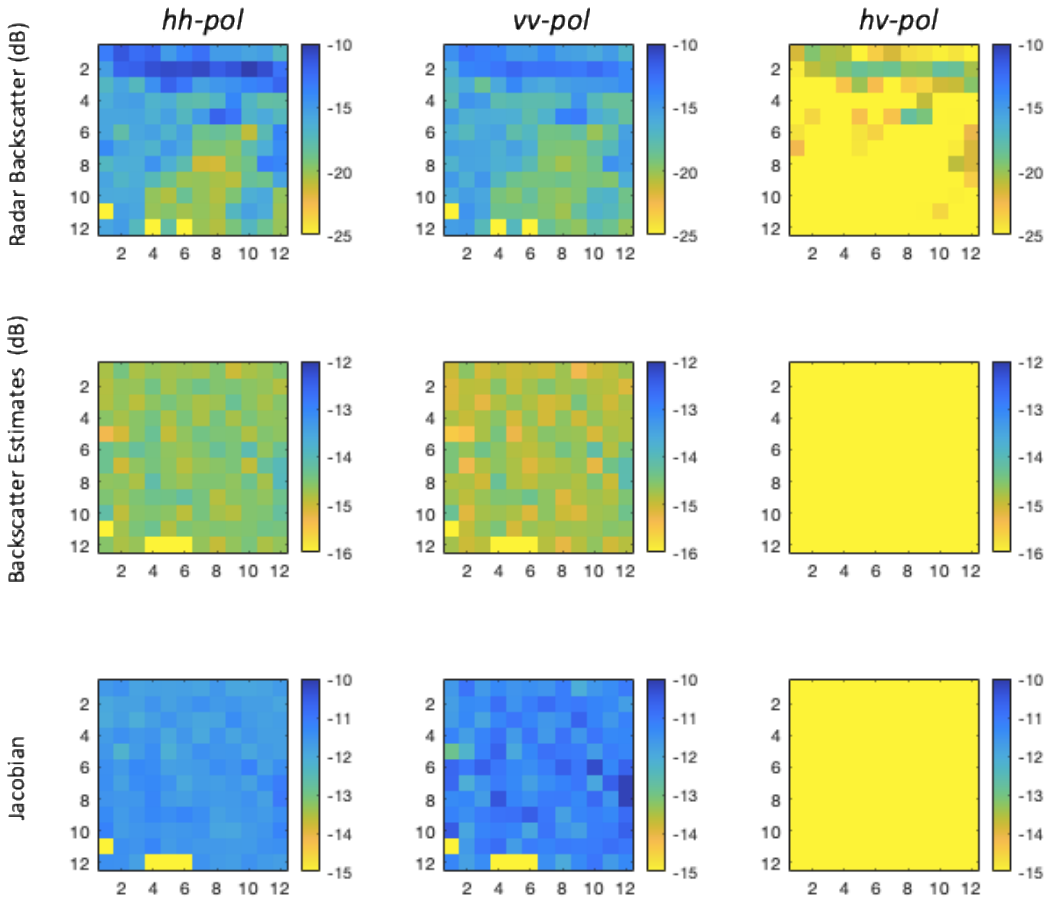

Figure 5: Example of the observed and estimated radar backscatter, and first derivatives (Jacobian) at *hh*-pol, *vv*-pol and *hv*-pol at 3 km resolution on D1, using the background soil moisture derived from the 36 km resolution SMAP radiometer on the same day.

diagonal elements of [*P*] was 0.052 cm^3/cm^3 across the 7 days of SMAPEx-4. Due to there being no true map of soil moisture at high resolution from SMAP, the downscaling procedure presented here relies on the estimated [*P*]. Nevertheless, in order to evaluate the influence of [*P*] estimation on the downscaling performance, the findings are juxtaposed with those obtained using the actual diagonal elements of [*P*].

The Bayesian downscaling was performed for each of the 7 days. Additionally, results at 9 km resolution were acquired through two methods, as described before, by: i) linearly upscaling the downscaled results at 3 km to 9 km; and ii) directly utilising the aggregated SMAP radar observations at 9 km resolution as the input rather than the original 3 km resolution. Only minor differences were found in terms of the downscaling accuracy between two methods, being less than 0.003 cm^3/cm^3. As a result, the following figures and statistics are all based on the linear aggregation approach.

To assess the performance of downscaling, three days (D1, D4, and D7) were selected from the full 7-day experimental period as an example. Those three days were selected as they captured the changes in vegetation and surface roughness throughout the entire SMAPEx-4 period. The downscaling results for the selected three days are in Figures 8-10, after excluding waterbodies and townships in a pre-processing step.

Upon comparison of the downscaled soil moisture with the reference map, it was observed that the downscaling error in the western areas of the SMAPEx-4 site was greater than in any other area, possibly owing to the influence of varying land cover types. The north-western area of the site, which was primarily used for cropping, exhibited greater variability in surface conditions including surface roughness, vegetation types and heights, biomass, and vegetation water content, as compared to the eastern area, which was predominantly covered by uniform grasslands. The non-uniform vegetation cover in the cropping-dominated western area affected the accuracy of radar observations in capturing the spatial distribution of soil moisture across the entire site, in contrast to the relatively homogeneous grassland in the eastern area. The impact of surface conditions on downscaling accuracy was found to decrease from 3 km to 9 km. As shown in Figure 2, the heterogeneity in vegetation and surface roughness, which affected the accuracy of the radar observations at 3 km, was effectively mitigated by pixel averaging at 9 km. Accordingly, the error in downscaling was reduced when applied at coarser resolutions. A comparison of the pattern

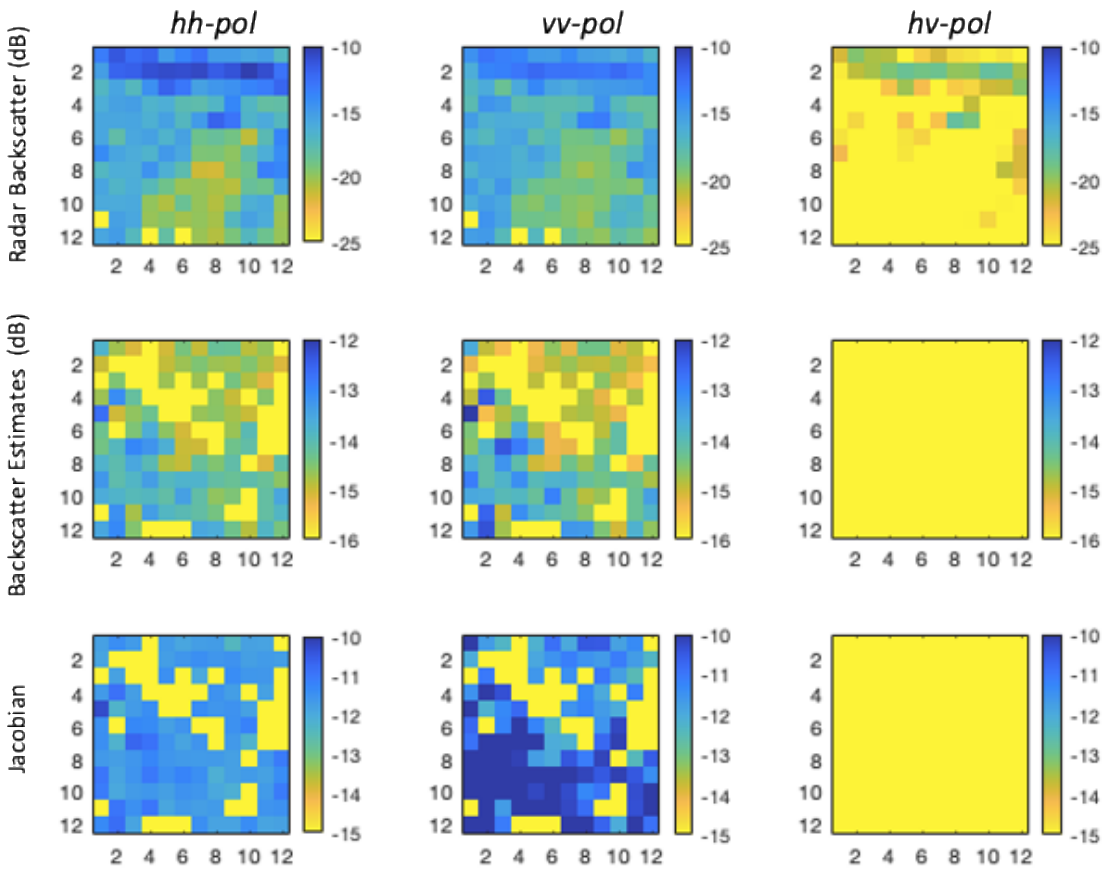

Figure 6: Example of the observed and estimated backscatter and first derivatives (Jacobian) at hh-pol, vv-pol and hv-pol at 3 km resolution on D1, using the background soil moisture derived from the SMAP radar on the same day.

matching between the downscaled soil moisture maps and reference maps revealed that the results for D7 were the poorest among the three selected days. The soil moisture variability was found to be higher across the SMAPEx site in the reference map shown in Figure 10 at a resolution of 3 km, which could be attributed to a rainfall event that occurred in the northeast region. Conversely, the results for D1 and D4 exhibited a better match with the reference map as compared to D7, since the heterogeneity across the site was reduced.

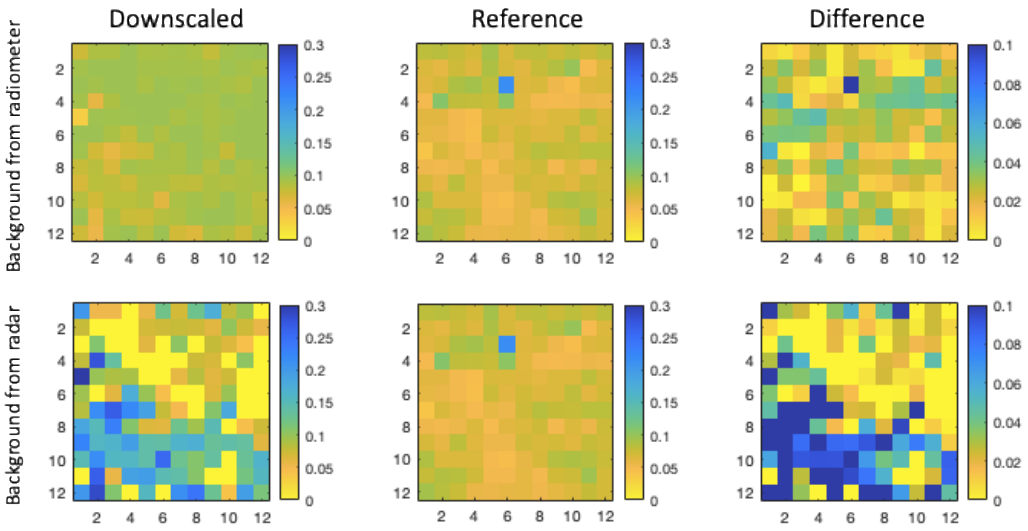

Figure 7: Spatial plots of downscaled soil moisture (cm^3/cm^3) and reference soil moisture (obtained from PLMR Tb via the single channel method) at 3 km resolution on D1, and the difference in soil moisture between those two. The background field was inversed either from 36 km resolution SMAP brightness temperature (*Tb*), or from 3 km resolution SMAP backscatter.

Results for the 7 days can be found in Table 4. It has been observed that towards the end of the campaign, there was an increase in the error of downscaling, which could be attributed to a corresponding increase in variation of the surface conditions (raining event in some part of study area near the end of the campaign). Results from the other two methods are also shown in Table 4. Accordingly, the SMAP baseline algorithm produced the least satisfactory results, due to a poor linear relationship and/or different patterns displayed by the radar and radiometer observations. The resolution enhancement method gave the next best results. While in this study the downscaling method that relied upon Bayes' Theorem and the enhancement method had a similar Mean Absolute Error (MAE), the Baseline method showed the largest average MAE across the 7 days. However, in terms of RMSE, the best results was found from the Bayesian method, with an improvement of approximately 0.058 cm^3/cm^3 over the baseline algorithm and 0.034 cm^3/cm^3 over the resolution enhancement method at 9 km resolution.

In addition to evaluating the performance on individual days, the three methods were compared by combining the results from all 7 days, as presented in Table 4 ("Combined"). The MAE, RMSE and correlation coefficient R^2 were obtained by comparing downscaled soil moisture to the reference soil moisture map over the 7-day period. Again, the baseline method demonstrated the weakest relationship between downscaled results and the reference soil moisture map.

Table 4

Comparison of downscaling results in terms of Root-Mean-Square-Error (RMSE, in cm^3/cm^3), Mean Absolute Error (MAE, in cm^3/cm^3) and Correlation Coefficient (R^2) at 9 km resolution across 7 days of SMAPEx-4 among three downscaling methods: SMAP Baseline algorithm, Bayesian merging method and SMAP Enhancement algorithm. Also shown are the "Average" and "Combined" RMSE and R^2 of all 7 days data.

		D1	**D2**	**D3**	**D4**	**D5**	**D6**	**D7**	**Average**	**Combined**
Baseline	RMSE	0.168	0.124	0.07	0.087	0.055	0.062	0.085	0.093	0.116
	R^2	0.12	0.28	0.45	0.52	0.38	0.29	0.41	0.35	0.38
	MAE	0.085	0.092	0.11	0.064	0.062	0.039	0.077	0.075	0.075
Bayesian	**RMSE**	**0.021**	**0.027**	**0.03**	**0.024**	**0.019**	**0.055**	**0.072**	**0.035**	**0.044**
	R^2	**0.38**	**0.52**	**0.58**	**0.46**	**0.61**	**0.63**	**0.66**	**0.55**	**0.61**
	MAE	**0.038**	**0.042**	**0.050**	**0.037**	**0.022**	**0.068**	**0.082**	**0.048**	**0.048**
Enhancement	RMSE	0.121	0.072	0.055	0.063	0.043	0.058	0.071	0.069	0.074
	R^2	0.41	0.46	0.31	0.65	0.43	0.47	0.21	0.41	0.44
	MAE	0.078	0.058	0.029	0.064	0.031	0.042	0.054	0.05	0.05

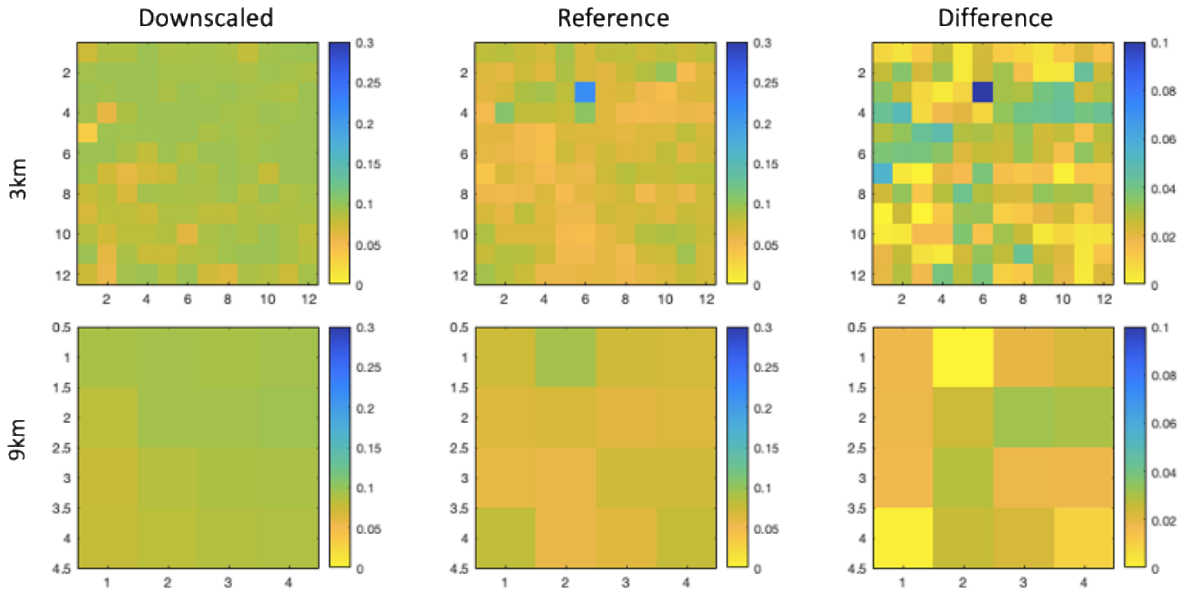

Figure 8: Spatial plots of downscaled soil moisture (cm^3/cm^3) from Bayesian merging algorithm, reference soil moisture map and their absolute differences at 3 km and 9 km resolution respectively. Data used here were collected from D1.

V. Discussion

The results above indicated that the supposition of a linear association between radiometer and radar data might require re-examination, particularly over mixed cropping areas. The resolution enhancement method had a slightly better performance over the baseline method, attributed to the fact that radiometer data is more correlated to soil moisture and less impacted from vegetation than radar. The 9 km resolution soil moisture achieved through the Bayesian merging algorithm exhibited an RMSE of approximately 0.035 cm^3/cm^3. Regarding correlation between the 9 km resolution downscaled product and the reference soil moisture map, the Baseline and Enhancement methods exhibited similar performance, while the Bayesian algorithm exhibited slightly better performance.

The spatial distribution of RMSE and R^2 has been analysed for all three methods by comparing downscaled soil moisture to the reference across the 7 days at each pixel. These results can be found in Figure 11. The resulting RMSE and R^2 across the entire study area indicated that the western region dominated by crops presented a higher RMSE and lower R^2 than the eastern grassland in Bayesian results, possibly attributed to the influence from vegetation characteristics and surface roughness parameter on radar observations. However, the discrepancy in RMSE and R^2 across the whole region decreased when the results were averaged to larger scales. Particularly at 9 km resolution, the Bayesian downscaling algorithm demonstrated some favourable outcomes.

Analysis and discussions above are all based on Type 1 or Type 2 background soil moisture, which only used the SMAP ancillary parameters over the Australian region. Given that the radiometer-based background had a better performance than the radar-based background, Type 4 was not actually considered, and thus only Type 3 (combining SMAP 36 km radiometer Tb and SMAPEx-4 field ancillary data) was actually tested. The resulting RMSE based on Type 3 was 0.029 cm^3/cm^3 (averaged) for the Bayesian merging method, confirming that an improved accuracy of ancillary data for estimating the background field does indeed have the potential to improve the downscaling performance.

V. Conclusion

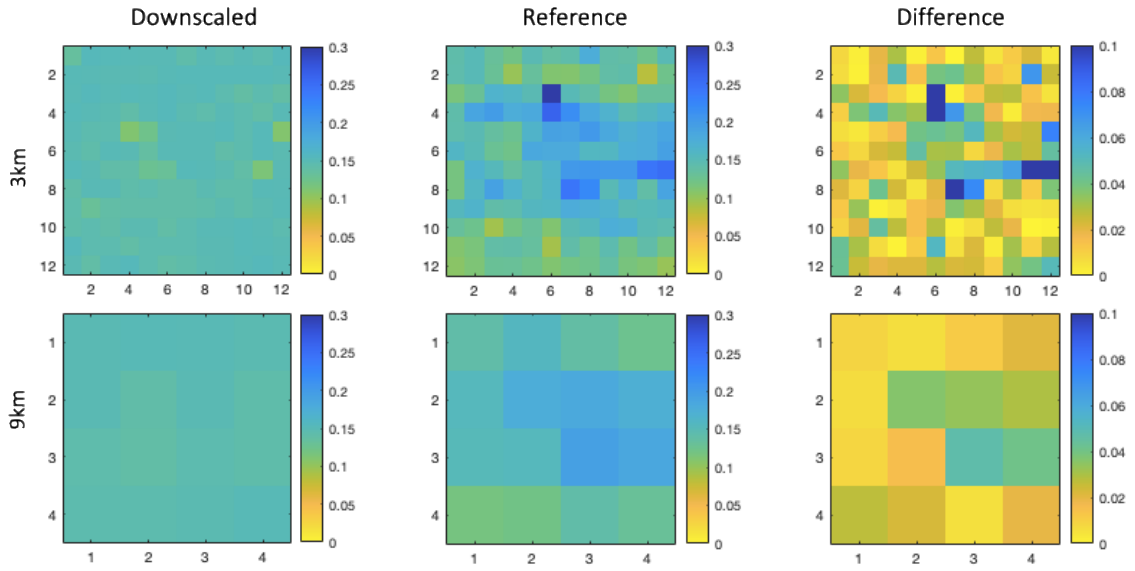

Figure 9: As for Figure 8 but on D4

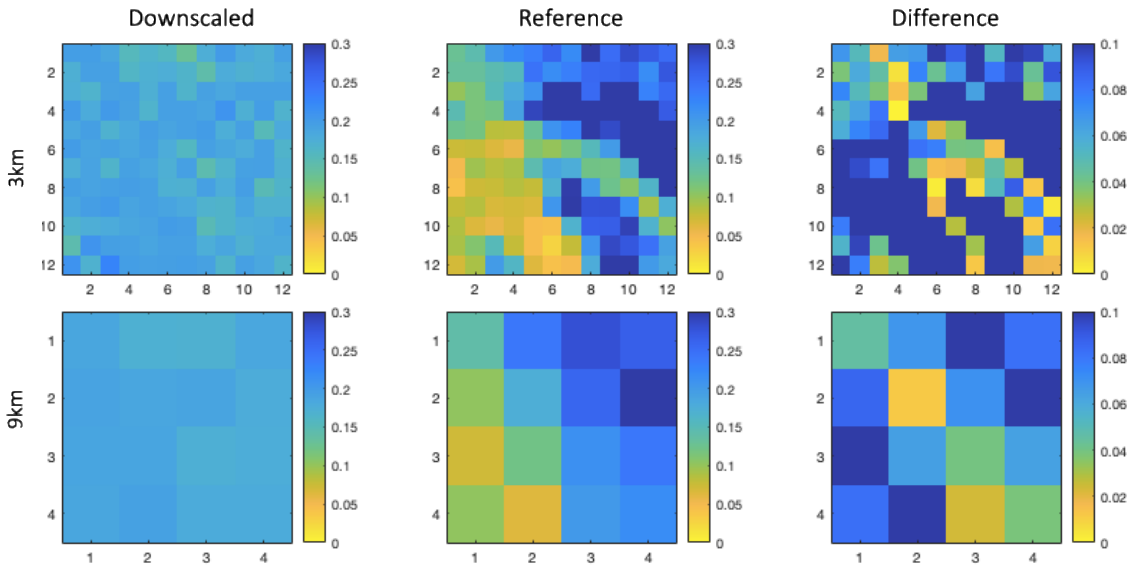

Figure 10: As for Figure 8 but on D7

The efficacy of the Bayesian merging approach as a medium-resolution soil moisture mapping technique was evaluated through the use of both coarse radiometer data and fine resolution radar data. Moreover, the applicability of this downscaling method to the SMAP satellite mission was evaluated in this study by utilizing real satellite data obtained from SMAP official active and passive products, and the field campaign named SMAPEx-4 conducted in Australia, in place of the synthetic data used during the development phase of the satellite mission. The accuracy of the Bayesian algorithm largely depends on the accuracy of radar-based inversion of soil moisture at high resolution. Accordingly, a more advanced radar retrieval algorithm is expected to further improve the performance of the Bayesian method. However, compared to other methods used for determining soil moisture at an intermediate resolution, the non-linear algorithm based on Bayes' theorem even with the radar model applied in this research exhibited superior outcomes in terms of RMSE and correlation R^2 at 9 km resolution, outperforming the SMAP official baseline algorithm and the resolution enhancement method. One potential drawback of the Bayesian algorithm as applied here was its reliance on default parameters during radar-based soil moisture retrieval. As such, it is believed that the adoption of a more sophisticated radar model would increase the Bayesian merging method's ability to produce a more accurate medium-resolution soil moisture product,

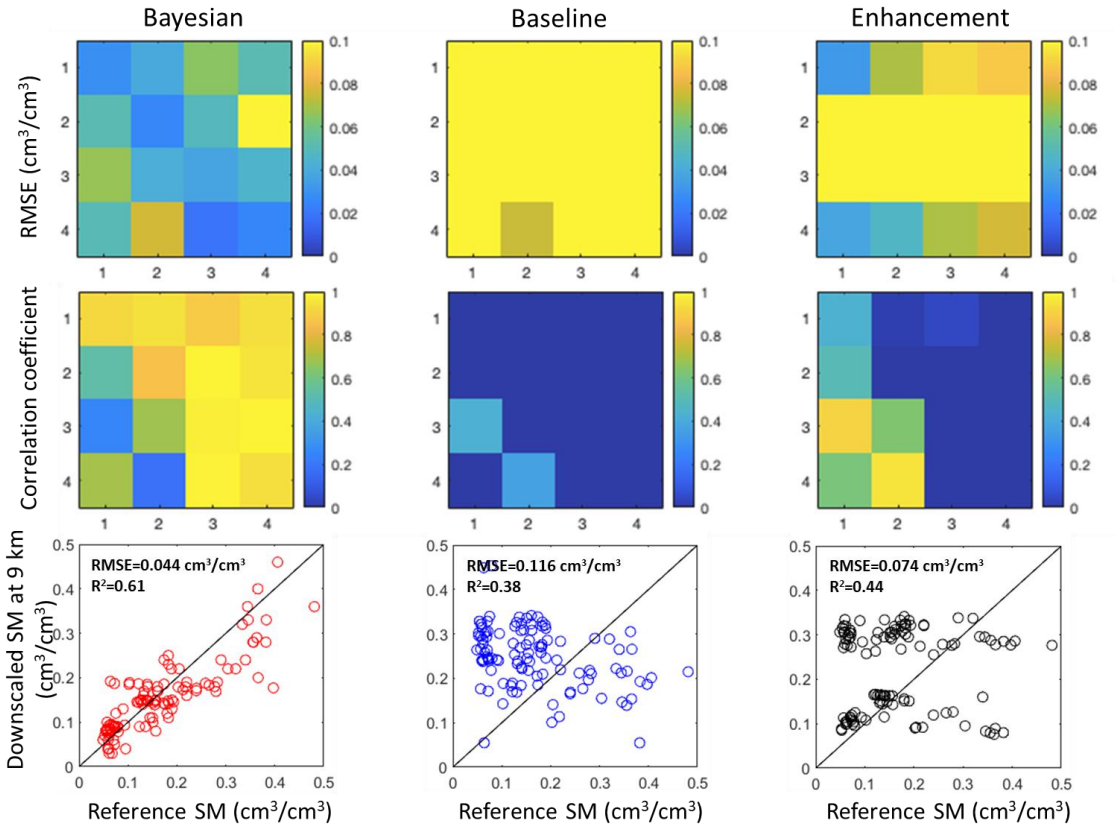

Figure 11: The spatial distribution of Root-Mean-Square-Error (RMSE, cm^3/cm^3) at top and correlation coefficient (R^2) at middle, and scatterplots between downscaled soil moisture (cm^3/cm^3) and reference soil moisture (cm^3/cm^3) for Bayesian merging method, SMAP baseline algorithm and SMAP enhancement algorithm at 9 km resolution. Result was calculated by comparing the downscaled soil moisture to the reference soil moisture map at each 9 km pixel across 7 days.

surpassing the performance of currently proposed alternative methods. Unfortunately, the SMAP radar failed shortly after launch and so the true value of using L-band radar for retrieving soil moisture has never been fully realised. It is anticipated that radar data from the series of SMAPEx field campaigns could contribute to the development and demonstration of radar soil moisture retrieval models, especially the availability of multi angular and multi temporal radar datasets which may help investigate the impact from vegetation and other surface conditions in future studies.

ACKNOWLEDGMENT

The series of SMAPEx field campaigns and associated research development were made possible through the support of Australian Research Council Discovery and Infrastructure grants (DP0984586, DP140100572, LE0453434, and LE0882509), and the collaboration from a diverse group of scientists from both Australia and the international community. The authors of this study would like to express their appreciation for this collaboration. They would also like to give special recognition to the key SMAP members who made significant contributions to the planning and implementation of the field campaign.

REFERENCES

[1] W. Wagner, K. Scipal, C. Pathe *et al.*, "Evaluation of the agreement between the first global remotely sensed soil moisture data with model and precipitation data," *Journal of Geophysical Research: Atmospheres*, vol. 108, no. D19, pp. 4611, 2003.

[2] Y. Kerr, "Soil moisture from space: Where are we?," *Hydrogeology Journal*, vol. 15, no. 1, pp. 117-120, 2007.

[3] Y. H. Kerr, P. Waldteufel, J. P. Wigneron *et al.*, "The SMOS Mission: New Tool for Monitoring Key Elements ofthe Global Water Cycle," *Proceedings of the IEEE*, vol. 98, no. 5, pp. 666-687, 2010.

[4] D. Entekhabi, E. G. Njoku, P. E. O'Neill *et al.*, "The Soil Moisture Active Passive (SMAP) Mission," *Proceedings of the IEEE*, vol. 98, no. 5, pp. 704-716, 2010.

[5] D. Entekhabi, N. N. Das, E. G. Njoku *et al.*, "Algorithm Theoretical Basis Document: L2 & L3 Radar/Radiometer Soil Moisture (Active/Passive) Data Products, Initial Release, v. 1," 2012.

[6] L. Brocca, W. Zhao, H. Lu. "High-resolution observations from space to address new applications in hydrology", *The Innovation*, vol. 4, no. 3, 2023.

[7] I. P. Senanayake, I. Y. Yeo, G. R. Willgoose, G. R. Hancock. "Disaggregating satellite soil moisture products based on soil thermal inertia: A comparison of a downscaling model built at two spatial scales", *Journal of Hydrology*, vol. 594, 2021.

[8] W. Zhao, F. Wen, Q. Wang, N. Sanchez, M. Piles. "Seamless downscaling of the ESA CCI soil moisture data at the daily scale with MODIS land products", *Journal of Hydrology*, vol. 603, Part B, 2021.

[9] O. Merlin, A. G. Chehbouni, Y. H. Kerr, E. G. Njoki & D. Entekhabi, "A combined modeling and multispectral/multiresolution remote sensing approach for disaggregation of surface soil moisture: application to SMOS configuration". *Geoscience and Remote Sensing, IEEE Transactions on*, 43, 2036-2050, 2005.

[10]N. N. Das, D. Entekhabi, and E. G. Njoku, "An Algorithm for Merging SMAP Radiometer and Radar Data for High-Resolution Soil-Moisture Retrieval," *IEEE Transactions on Geoscience and Remote Sensing*, vol. 49, no. 5, pp. 1504-1512, 2011.

[11]N. N. Das, D. Entekhabi, E. G. Njoku *et al.*, "Tests of the SMAP Combined Radar and Radiometer Algorithm Using Airborne Field Campaign Observations and Simulated Data," *IEEE Transactions on Geoscience and Remote Sensing*, vol. 52, no. 4, pp. 2018-2028, 2014.

[12]M. Piles, D. Entekhabi, and A. Camps, "A Change Detection Algorithm for Retrieving High-Resolution Soil Moisture From SMAP Radar and Radiometer Observations," *IEEE Transactions on Geoscience and Remote Sensing*, vol. 47, no. 12, pp. 4125-4131, 2009.

[13]X. Wu, J. P. Walker, C. Rüdiger *et al.*, "Intercomparison of Alternate Soil Moisture Downscaling Algorithms Using Active-Passive Microwave Observations," *IEEE Geoscience and Remote Sensing Letters*, vol. PP, no. 99, 2016. DOI: 10.1109/LGRS.2016.2633521

[14]X. Zhan, P. R. Houser, J. P. Walker *et al.*, "A method for retrieving high-resolution surface soil moisture from hydros L-band radiometer and radar observation," *IEEE Transactions on Geoscience and Remote Sensing*, vol. 44, no. 6, pp. 1534-1544, 2006.

[15]R. Panciera, J. P. Walker, T. J. Jackson *et al.*, "The Soil Moisture Active Passive Experiments (SMAPEx): Toward Soil Moisture Retrieval From the SMAP Mission," *IEEE Transactions on Geoscience and Remote Sensing*, vol. 52, no. 1, pp. 490-507, 2014.

[16]X. Wu, J. P. Walker, C. Rüdiger *et al.*, "Simulation of the SMAP Data Stream from SMAPEx Field Campaigns in Australia," *IEEE Transactions on Geoscience and Remote Sensing*, vol. 53, no. 4, pp. 1921-1934, 2015.

[17]R. E. Kalman, "A New Approach to Linear Filtering and Prediction Problems," *Transactions of the ASME – Journal of Basic Engineering*, no. 82 (Series D), pp. 35-45, //, 1960.

[18]J. Wigneron, A. Chanzy, Y. H. Kerr *et al.*, "Evaluating an Improved Parameterization of the Soil Emission in L-MEB," *Geoscience and Remote Sensing, IEEE Transactions on*, vol. 49, no. 4, pp. 1177-1189, 2011.

[19]R. Panciera, J. P. Walker, J. D. Kalma *et al.*, "Evaluation of the SMOS L-MEB passive microwave soil moisture retrieval algorithm," *Remote Sensing of Environment*, vol. 113, no. 2, pp. 435-444, 2009.

[20]P. C. Dubois, J. Van Zyl, and T. Engman, "Measuring soil moisture with imaging radars," *Geoscience and Remote Sensing, IEEE Transactions on*, vol. 33, no. 4, pp. 915-926, 1995.

[21]Y. Oh, K. Sarabandi, and F. T. Ulaby, "An empirical model and an inversion technique for radar scattering from bare soil surfaces," *Geoscience and Remote Sensing, IEEE Transactions on*, vol. 30, no. 2, pp. 370-381, 1992.

[22]J. R. Wang, and T. J. Schmugge, "An Empirical Model for the Complex Dielectric Permittivity of Soils as a Function of Water Content," *Geoscience and Remote Sensing, IEEE Transactions on*, vol. GE-18, no. 4, pp. 288-295, 1980.

[23]Y. Gao, J. P. Walker, N. Ye *et al.*, "Evaluation of the Tau-Omega Model for Passive Microwave Soil Moisture Retrieval using SMAPEx Data Sets," *IEEE Journal of Seleced Topics in Applied Earth Observations and Remote Sensing*, vol. 11, pp. 888-895, 2018.

[24] X. Wu, J. P. Walker, C. Rüdiger, R. Panciera and Y. Gao, "Medium-Resolution Soil Moisture Retrieval Using the Bayesian Merging Method," *IEEE Transactions on Geoscience and Remote Sensing*. vol. 55, no. 11, pp. 6482-6493, 2017.